



# Activity of Estrogen Receptor $\beta$ Agonists in Therapy-Resistant Estrogen Receptor-Positive Breast Cancer

## OPEN ACCESS

### Edited by:

Ke-Da Yu,  
Fudan University, China

### Reviewed by:

Jianchun Wu,  
University of Illinois at Chicago,  
United States  
Takahiro Kogawa,  
Cancer Institute Hospital of Japanese  
Foundation for Cancer Research,  
Japan  
Carlos Martinez-Perez,  
Medical Research Council Institute of  
Genetics and Molecular Medicine  
(MRC), United Kingdom

### \*Correspondence:

Mathew A. Cherian  
mathew.cherian@osumc.edu

### Specialty section:

This article was submitted to  
Breast Cancer,  
a section of the journal  
Frontiers in Oncology

**Received:** 18 January 2022

**Accepted:** 28 February 2022

**Published:** 25 April 2022

### Citation:

Datta J, Willingham N,  
Manouchehri JM, Schnell P,  
Sheth M, David JJ, Kassem M,  
Wilson TA, Radomska HS, Coss CC,  
Bennett CE, Ganju RK, Sardesai SD,  
Lustberg M, Ramaswamy B, Stover DG  
and Cherian MA (2022) Activity of  
Estrogen Receptor  $\beta$  Agonists in  
Therapy-Resistant Estrogen  
Receptor-Positive Breast Cancer.  
*Front. Oncol.* 12:857590.  
doi: 10.3389/fonc.2022.857590

Jharna Datta<sup>1</sup>, Natalie Willingham<sup>1</sup>, Jasmine M. Manouchehri<sup>1</sup>, Patrick Schnell<sup>1,2</sup>,  
Mirisha Sheth<sup>1</sup>, Joel J. David<sup>1</sup>, Mahmoud Kassem<sup>1,2</sup>, Tyler A. Wilson<sup>1,3</sup>, Hanna S. Radomska<sup>4</sup>,  
Christopher C. Coss<sup>1,4,5</sup>, Chad E. Bennett<sup>1,3,5</sup>, Ramesh K. Ganju<sup>1</sup>, Sagar D. Sardesai<sup>1,2</sup>,  
Maryam Lustberg<sup>6</sup>, Bhuvanewari Ramaswamy<sup>1,2</sup>, Daniel G. Stover<sup>1,2</sup> and Mathew A. Cherian<sup>1,2\*</sup>

<sup>1</sup> Comprehensive Cancer Center, The Ohio State University Wexner Medical Center, Columbus, OH, United States, <sup>2</sup> Stefanie Spielman Comprehensive Breast Cancer, The Ohio State University, Columbus, OH, United States, <sup>3</sup> Medicinal Chemistry Shared Resource, Comprehensive Cancer Center, The Ohio State University Wexner Medical Center, Columbus, OH, United States, <sup>4</sup> Division of Pharmaceutics and Pharmacology, College of Pharmacy, The Ohio State University, Columbus, OH, United States, <sup>5</sup> Drug Development Institute, The Ohio State University, Columbus, OH, United States, <sup>6</sup> Yale Cancer Center, Yale School of Medicine, New Haven, CT, United States

**Background:** Among women, breast cancer is the leading cause of cancer-related death worldwide. Estrogen receptor  $\alpha$ -positive (ER $\alpha$ +) breast cancer accounts for 70% of all breast cancer subtypes. Although ER $\alpha$  breast cancer initially responds to estrogen deprivation or blockade, the emergence of resistance compels the use of more aggressive therapies. While ER $\alpha$  is a driver in ER $\alpha$  breast cancer, ER $\beta$  plays an inhibitory role in several different cancer types. To date, the lack of highly selective ER $\beta$  agonists without ER $\alpha$  activity has limited the exploration of ER $\beta$  activation as a strategy for ER $\alpha$  breast cancer.

**Methods:** We measured the expression levels of *ESR1* and *ESR2* genes in immortalized mammary epithelial cells and different breast cancer cell lines. The viability of ER $\alpha$  breast cancer cell lines upon treatments with specific ER $\beta$  agonists, including OSU-ERb-12 and LY500307, was assessed. The specificity of the ER $\beta$  agonists, OSU-ERb-12 and LY500307, was confirmed by reporter assays. The effects of ER $\beta$  agonists on cell proliferation, cell cycle, apoptosis, colony formation, cell migration, and expression of tumor suppressor proteins were analyzed. The expression of *ESR2* and genes containing ERE-AP1 composite response elements was examined in ER $\alpha$  human breast cancer samples to determine the correlation between *ESR2* expression and overall survival and that of putative *ESR2*-regulated genes.

**Results:** In this study, we demonstrate the efficacy of highly selective ER $\beta$  agonists in ER $\alpha$  breast cancer cell lines and drug-resistant derivatives. ER $\beta$  agonists blocked cell proliferation, migration, and colony formation and induced apoptosis and S and/or G2/M cell-cycle arrest of ER $\alpha$  breast cancer cell lines. Also, increases in the expression of the

key tumor suppressors FOXO1 and FOXO3a were noted. Importantly, the strong synergy between ER $\beta$  agonists and ER $\alpha$  antagonists suggested that the efficacy of ER $\beta$  agonists is maximized by combination with ER $\alpha$  blockade. Lastly, *ESR2* (ER $\beta$  gene) expression was negatively correlated with *ESR1* (ER $\alpha$  gene) and *CCND1* RNA expression in human metastatic ER $\alpha$ + /HER2- breast cancer samples.

**Conclusion:** Our results demonstrate that highly selective ER $\beta$  agonists attenuate the viability of ER $\alpha$ + breast cancer cell lines *in vitro* and suggest that this therapeutic strategy merits further evaluation for ER $\alpha$ + breast cancer.

**Keywords:** ER $\alpha$ , ER $\beta$ , ER+ breast cancer, OSU-ERb-12, LY500307

## INTRODUCTION

Breast cancer is the most prevalent cancer among women globally (1). It is the second leading cause of cancer-related deaths among women. In 2020, there were 2.3 million new breast cancer cases and 685,000 breast cancer deaths worldwide. Despite advances in diagnostic procedures and improved therapies, globally breast cancer-related morbidity and mortality are on the rise. The majority of breast cancer-related deaths occur due to distant metastasis. About 60% of metastatic breast cancers (MBC) are estrogen receptor  $\alpha$  positive (ER $\alpha$ +) and human epidermal growth factor receptor 2 non-amplified (HER2-) (2). Although the development of effective estrogen blocking agents and cyclin-dependent kinase 4/6 inhibitors (CDK4/6i) has doubled progression-free survival on first-line therapy of ER $\alpha$ + -HER2- MBC, endocrine and CDK4/6i resistance emerges causing disease progression. Appropriate post-CDK4/6i therapy is poorly defined due to an incomplete understanding of CDK4/6i resistance, lack of effective agents, and lack of clinical trials that address this important issue.

While augmented signaling through receptor tyrosine kinases, *NF1* loss, *C-MYC* amplification, and activating mutations in the *ESR1* gene result in endocrine resistance, alterations of cell-cycle genes cause CDK4/6i resistance (3–5). Due to redundancy and cross talk in these signaling pathways, attempts to counter therapeutic resistance by focusing on a single target have been mostly ineffective. Thus, there is an urgent need to develop novel therapeutic options in the second-line setting to improve the survival and response rate for aggressive endocrine and CDK4/6i-resistant MBC.

Estrogens play a vital role in breast tumorigenesis (6, 7). The stimulatory or repressive effects of estrogens are mediated through ER $\alpha$  and ER $\beta$ , which are gene products of *ESR1* and *ESR2*, respectively, and the G protein-coupled estrogen receptor (GPCR30). Unlike ER $\alpha$ , which has a clear oncogenic role in ER $\alpha$ + breast cancer, ER $\beta$  behaves like a tumor suppressor in many biological contexts. For example, the tumor-suppressive function of ER $\beta$  was demonstrated through its knockdown in ER $\alpha$ + cell lines, which induced an invasive phenotype, increased anchorage-dependent cell proliferation, and elevated EGF-R signaling (8). In the presence of estradiol, ER $\beta$  overexpression reduced cell proliferation *in vitro* and tumor formation *in vivo*, effects that are in contradistinction to those of ER $\alpha$  (9, 10).

In these experiments, ER $\beta$  was also shown to repress the expression of oncogenes such as *c-myc* and *cyclin D1* (*CCND1*).

The transcriptional function of ERs involves their binding to estrogen response elements (ERE) within promoters and enhancers (11). There are multiple conformations of EREs in the human genome, including consensus and non-consensus EREs, single and multiple binding sites, and composite EREs consisting of ERE half-sites in combination with binding sites for other transcription factors such as AP1 and Sp1. Although both the receptors exhibit transcriptional activity, they differ in their modes of transcriptional activation (12). Studies demonstrated that on certain E2-responsive ERE-AP-1 composite promoters, ER $\beta$  actually antagonizes the effects of ER $\alpha$  (13). For example, the *CCND1* promoter, containing a cAMP response element and an AP-1-binding site, is activated by estradiol in cells overexpressing ER $\alpha$  but is inhibited in cells overexpressing ER $\beta$  (13).

*ESR2* was discovered more than 20 years ago (14), but its clinical application was limited by the lack of highly selective ER $\beta$  agonists. Although both ER $\alpha$  and ER $\beta$  are activated by binding to endogenous estrogens, the development of several highly selective synthetic ligands of ER $\alpha$  or ER $\beta$  has uncovered new avenues to probe the function of these receptors (15).

In the present study, we investigated the effects of a novel and highly selective ER $\beta$ -selective agonist, OSU-ERb-12 (16), to inhibit preclinical models of ER $\alpha$ + breast cancer and to counter endocrine and CDK4/6i resistance *in vitro*. We found that treatment of ER $\alpha$ + breast cancer cell lines with OSU-ERb-12 caused apoptosis, induced cell-cycle arrest (at S phase), and decreased cell proliferation, colony formation, and cell migration. FOXO1 and FOXO3a protein expression was significantly increased in cells treated with OSU-ERb-12, a potential mechanism for its tumor-suppressive effects (17).

## MATERIALS AND METHODS

### Chemicals, Drugs, Plasmids, Antibodies, Primers, and Synthesis of MCSR-18-006

OSU-ERb-12 was synthesized in the Drug Development Institute (DDI) at OSU according to the procedure outlined before (16). LY500307 was also obtained from DDI, OSU. AC186 (cat# 5053), WAY200076 (cat# 3366), diarylpropionitrile (DPN; cat# 1494), 4-hydroxy-tamoxifen (Tam; cat# 3412/10), fulvestrant

(Fas; cat# 10-471-0), and 1,3-bis(4-hydroxyphenyl)-4-methyl-5-[4-(2-piperidinyloxy)phenol]-1H-pyrazoledihydro-chloride (MPP; cat# 1991) were purchased from Tocris Bioscience (Bristol, UK). Elacestrant (RAD1901; cat# S9629) was purchased from Selleckchem (Houston, TX, USA). Abemaciclib (LY2835219; cat# 17740) was obtained from Cayman Chemical (Ann Arbor, MI, USA). Stock solutions (10 mmol/l) of the inhibitors were prepared in DMSO. CellTiter-Glo reagent (cat# G7570) and Dual-Luciferase Assay reagent (cat# E1960) were purchased from Promega Corporation (Madison, WI, USA). Lipofectamine 3000 was obtained from Thermo Fisher Scientific (Waltham, MA, USA).

*pRLTK* plasmid was obtained from Promega. *3XERE TATA luc* (luciferase reporter that contained three copies of vitellogenin estrogen response element) was a kind gift from Donald McDonnell (Addgene plasmid # 11354; <http://n2t.net/addgene:11354>; RRID: Addgene\_11354). Plasmids *pcDNA3* (OHu23619C; *pcDNA3.1+*; RRID: Addgene\_10842), ER $\beta$  (OHu25562C; *pcDNA3.1+*), c-Flag *pcDNA3* (OHu23619D; *pcDNA3.1+/C-(K) DYK*), c-Flag ER $\alpha$  (OHu26586D; *pcDNA3.1+/C-(K) DYK*), and c-Flag ER $\beta$  (OHu25562D; *pcDNA3.1+/C-(K) DYK*) were obtained from GenScript (Piscataway, NJ, USA).

Antibodies to ER $\alpha$  (D8H8; 8644), FOXO1 (D7C1H; cat# 14952, RRID : AB\_2722487), FOXO3a (75D8; cat# 2497), PARP (cat# 9542, RRID : AB\_2160739), cleaved PARP (Asp24, D64E10; cat# 5625, RRID : AB\_10699459), caspase-3 (8G10; cat# 9665, RRID : AB\_2069872), cleaved caspase-3 (D175; cat# 9664, RRID : AB\_2070042), caspase-7 (cat# 9492, RRID : AB\_2228313), cleaved caspase-7 (asp198, D6H1; cat# 8433, RRID : AB\_11178377), and GAPDH (D16H11; cat# 8884, RRID : AB\_11129865) were obtained from Cell Signaling Technology (Danvers, MA, USA). Antibodies against ER $\beta$  (clone 68-4; cat# 05-824) and M2 Flag (cat# F1804) were purchased from Sigma-Aldrich (St. Louis, MO, USA).

The following primers were used for the corresponding mRNAs. *ESR2* full length: forward (5'-CTCCAGATCTTGT TCTGGACAGGGAT-3'), reverse (5'-GTTGAGCAGATGTTC CATGCCCTTGTTA-3'); *ESR2* all isoforms: forward (5'-ACA CACCTTACCTGTAAACAGAGAG-3'), reverse (5'-GGG AGCCACACTTCACCATTC-3'); *ESR1*: forward (5'-CCGCC GGCATTCTACAGGCC-3'), reverse (5'-GAAGAAGGCCTTG C AGCCCT-3'); *GAPDH*: forward (5'-GTCGTATTGGCGCCT GGTC-3'), reverse (5'-TT TGGAGGGATCTCGTCCT-3').

<sup>1</sup>H-NMR spectra were recorded using a Bruker AV300NMR, AVIII400HD NMR spectrometer or a DRX400 NMR spectrometer at The Ohio State University College of Pharmacy. Chemical shifts ( $\delta$ ) are specified in ppm from chemical reference shifts for internal deuterated chloroform (CDCl<sub>3</sub>) set to 7.26 ppm. Coupling constants are defined in Hz. Mass spectra were obtained using an Advion Expression Model S Compact Mass Spectrometer equipped with an APCI source and TLC plate express or using a Thermo LTQ Orbitrap mass spectrometer. For carborane-containing compounds, the obtained mass resembling the most intense peak of the theoretical isotopic pattern was described. Measured patterns corresponded with calculated patterns. Unless otherwise noted, all reactions were carried out under argon atmosphere using commercially available reagents and solvents. Details of the

procedure for the synthesis of MCSR-18-006 are provided in **Supplemental Data**.

## Cell Culture, Cell Viability, and Generation of Resistance

Immortal mammary epithelial cells MCF10A (ATCC Cat# CRL-10317, RRID : CVCL\_0598) and breast cancer cell lines MCF7 (ATCC HTB-22), T47D (ATCC HTB-133; NCI-DTP Cat# T-47D, RRID : CVCL\_0553), ZR-75-1 (ATCC CRL-1500), MDA-MB 231 (ATCC HTB-26, RRID : CVCL\_0062), MDA-MB 468 (ATCC HTB-132, RRID : CVCL\_0419), and HEK-293T (ATCC Cat# CRL-3216, RRID : CVCL\_0063) were obtained from ATCC. All the cells were grown according to the supplier's recommendation in a humidified atmosphere containing 5% CO<sub>2</sub> at 37°C. Cells were passaged and media changed every 2 days. Mycoplasma contamination of the cells were checked monthly using the MycoAlert Plus Mycoplasma Detection Kit (cat# LT07-703) (Lonza, Walkersville, MD, USA) following the manufacturer's protocol. For routine experiments, parental and drug-resistant cells of MCF7 and T47D were cultured in phenol red-free basal medium (DMEM) media, containing charcoal-stripped fetal bovine serum (10%), L-glutamine (2 mM), Napyruvate (1 mM), penicillin (100 units), and streptomycin (100 units).

Resistant MCF7 (MCF7-TamR and MCF7-FasR) cells were gifts from Dr. Kenneth Nephew (18). In addition, the MCF7 cell line that overexpresses CDK6 (MCF7-CDK6 O/E), which has previously been described and is resistant to abemaciclib, was a gift from Sarat Chandralapaty, Memorial Sloan Kettering Cancer Center (19). T47D cells were treated at gradually increasing concentrations with 4-hydroxy-tamoxifen (Tam), fulvestrant/Faslodex (Fas; estrogen receptor antagonist) or abemaciclib (cyclin-dependent kinase 4/6 inhibitor; CDK4/6i) to generate resistant cell lines (T47D-TamR, T47D-FasR, and T47D-CDK4/6iR). Similarly, MCF7 cells were treated with increasing concentrations of abemaciclib to generate MCF7-CDK4/6iR cells. Control cells were treated with the vehicle DMSO. The starting concentrations of the drugs ranged from 25 to 50 nmol/l and increased stepwise every 2–3 weeks. To evaluate the development of resistance, cells (both control and drug-treated) were examined for viability every 4 to 6 weeks with the CellTiter-Glo assay (Promega). Unless stated otherwise, cell viability was measured in quadruplicates by seeding the cells (2,000 to 3,000 per well in 96-well plate), followed by addition of Tam, Fas, or abemaciclib at different dilutions or DMSO (vehicle control) after 24 h. Seventy-two hours later, luminescence was measured after the addition of CellTiter-Glo reagent following the manufacturer's protocol. Cell viability was calculated as percentage relative to vehicle controls (100%). Sigmoidal dose-response curves were plotted using GraphPad Prism software (GraphPad Prism, RRID: SCR\_002798). Upon manifesting resistance, cells were maintained with continued drug exposure at concentrations to which they were resistant.

Immortal mammary epithelial MCF10A cells as well as MCF7 and T47D breast cancer (parental and respective resistant) cells were allowed to grow overnight followed by treatment with OSU-

ERb-12, LY500307, DPN (diarylpropionitrile), AC186, and WAY200070 (WAY) at varying concentrations as indicated. The fresh medium and drugs were replaced every alternate day. Cell viability was assessed after 7 days of initial drug exposure using CellTiter-Glo Luminescent Cell Viability Assay, and the viability curves were plotted as mentioned above.

### Reverse Transcription Polymerase Chain Reaction, Western Blot Analysis, Estrogen Response Element Luciferase Reporter Assays, and Messenger RNA Expression Analysis of Patient Samples

Total RNA was isolated from cells using TRIzol reagent (cat# 15596026) (Invitrogen, Carlsbad, CA) following the manufacturer's instructions, treated with DNase I, and reverse transcribed into cDNA using the high-capacity cDNA reverse transcription kit (Applied Biosystems, Foster City, CA). Real-time RT-PCR (qRT-PCR) was performed using 0.01–0.05 μg cDNA with SYBR Green Master Mix (Applied Biosystems, Foster City, CA, USA) in an Applied Biosystems thermocycler. The fold difference in target gene mRNA levels normalized to GAPDH was calculated using the  $\Delta\Delta CT$  method. Semiquantitative PCR was performed using the same set of primers as in qRT-PCR and visualized after electrophoretic separation to confirm the identity of the amplicons. The primers were designed spanning the exon-exon junction to avoid non-specific amplification of genes.

Whole-cell extracts were prepared in cell lysis buffer (50 mM Tris pH 8.1, 10 mM EDTA, 1% SDS, and 1% IGEPAL CA-630; cat# 18896, Sigma-Aldrich) followed by sonication and centrifugation at 14,000 rpm for 10 min at 4°C. Protein concentrations in the extracts were measured using the bicinchoninic acid (BCA) method using BSA as the standard. Equivalent amounts of protein from whole-cell lysates were mixed with 4× Laemmli's buffer, boiled for 5 min at 97°C, separated by SDS-polyacrylamide (10%) gel electrophoresis (Thermo Fisher Scientific), transferred to nitrocellulose membranes (GE Healthcare, Chicago, IL), and probed with the antibodies described above. Membranes were incubated overnight at 4°C with the primary antibody, washed, and blotted for an hour with secondary anti-mouse/rabbit (HRP-conjugated) antibodies. The enhanced chemiluminescence substrate detection system (Millipore-Sigma) was applied to detect bound antibody complexes and visualized by autoradiography. The loading control was GAPDH. The intensity of the protein bands was quantified using Image Studio (LiCor).

HEK293T cells ( $7.5 \times 10^4$ /well) seeded in a 24-well plate were transfected for 12 h with *ERE-Luc*, *pRLTK* (internal control, Promega), and *c-Flag pcDNA3/ERα/ERβ* plasmids using Lipofectamine 3000 (Thermo Fisher Scientific) following the manufacturer's protocol. The media were changed with phenol-free DMEM containing 10% charcoal-stripped FBS and insulin (6 ng/ml). Six hours later, cells were treated with OSU-ERb-12 or LY500307 at varying concentrations as indicated. DMSO was used as a vehicle control. Luciferase activity was assessed after 72 h of transfection using Dual-Luciferase Assay System (Promega).

Patients treated at The Ohio State University Comprehensive Cancer Center – Arthur G. James Cancer Hospital and Richard J.

Solove Research Institute since 1998 with a diagnosis of metastatic ERα+ and HER2-negative (ERα+/HER2-) breast cancer and confirmed RNA sequencing analysis were eligible for this retrospective clinical correlation. Following IRB approval (OSU protocol No: 2018C0211), the list of patients fulfilling the previous criteria was obtained from the Ohio State University Medical Center and James Cancer Registry. 118 medical record were reviewed, and 37 patients had RNA sequencing performed through the Oncology Research Information Exchange Network (ORIEN) and were deemed eligible.

Data for the 37 eligible patients were initially queried and obtained from The Ohio State University Information Warehouse and from ORIEN-AVATAR and uploaded into REDCap (REDCap, RRID : SCR\_003445). Data missing from the initial query were populated using a manual review of each patient's electronic medical record.

Total RNA was sequenced with minimum 20 million reads and >65% reads aligned identified for subsequent processing to transcript abundance values (FKPM; fragments per kilobase per million reads) following the ORIEN standard pipeline: STAR aligner (STAR, RRID : SCR\_004463), Star-fusion, and RSEM (RSEM, RRID : SCR\_013027) with genome GRCh38 alignment/annotation.

### Cell Proliferation, Cell Cycle Analysis, Apoptosis, Clonogenic Survival, and Cell Migration Assays

MCF7 and T47D cells were plated at  $5 \times 10^5$  cells per plate in phenol red-free complete DMEM supplemented with charcoal-stripped FBS. Twenty-four hours later, the cells were treated for 72 h with OSU-ERb-12 (0.5 and 10 μmol/l) or LY500307 (MCF7: 0.5 and 3 μmol/l; T47D: 0.5 and 7 μmol/l). Differing concentrations were used to avoid complete loss of viability. DMSO and fulvestrant (0.5 μmol/l) were used as negative and positive controls, respectively. The cells were harvested and stained as per the protocol for the Click-iT EdU Alexa Fluor 647 Kit (Invitrogen; cat# C10424). The stained cells were analyzed *via* flow cytometry (BD FACSCalibur Flow Cytometer).

For cell-cycle analysis, MCF7 and T47D cells were plated and treated for 72 h with OSU-ERb-12 or LY500307 at the indicated concentrations. DMSO was used as vehicle control. The cells were harvested, fixed in 70% ethanol, and stained with propidium iodide. The stained cells were analyzed *via* flow cytometry on a BD FACSCalibur Flow Cytometer.

Breast cancer MCF-7 and T47D cells were plated and treated 24 h later with OSU-ERb-12 (0.5 and 10 μmol/l) or LY500307 (MCF7: 0.5 and 3 μmol/l; T47D: 0.5 and 7 μmol/l) for 48 h. Cells were collected and processed according to the manufacturer (TUNEL Assay Kit - BrdU-Red (cat# ab66110) (Abcam, Cambridge, MA, USA). Processed breast cancer cells were analyzed on a BD FACSCalibur Flow Cytometer to determine the percentage of apoptotic cells in each treatment group.

MCF7 and T47D cells were plated in 60-mm dishes (~1,000–2,000 cells). Twenty-four hours after plating, cells were treated with OSU-ERb-12, LY500307, or vehicle (DMSO) for 7–10 days. The fresh medium and drugs were replaced every other day. Next, cell colonies were washed with PBS, fixed with paraformaldehyde (4%),

and stained with crystal violet solution (0.05%). Colonies were then washed with water and air-dried. Visible colonies were counted manually.

For cell migration assay, MCF7 cells were seeded, treated with DMSO (control), OSU-ERb-12, or LY500307 and allowed to grow until confluence. Confluent monolayers were scratched using a sterile pipette tip, washed, and incubated in complete medium containing DMSO or the drugs. Plates with similar scratch were selected by examination under microscope and used for further analysis. Images were captured immediately after scratch (0 h) and 24 h post-scratch. Migration of cells from the edge of the groove toward the center was monitored at 24 h ( $\times 40$  magnification). To calculate the fraction of the gap covered by the cells in a 24-h period, the width of the scratch was measured at 0 h and at 24 h. The mean fraction of the filled area was determined, and data presented were normalized to the control cells.

## Statistical and Bioinformatics Analyses

Viability, proliferation, apoptosis, and cellular mRNA expression were analyzed using student's t-test. For each dose, linear mixed models were fit for log-transformed viability with fixed effects for regimen (4-hydroxy-tamoxifen, OSU-ERb-12, and 4-hydroxy-tamoxifen+OSU-ERb-12) and random effects accounting for the within-batch correlation of replicates. Predictions and standard errors for viability of the 4-hydroxy-tamoxifen+OSU-ERb-12 combination under a hypothesized Bliss independence model were computed from estimated mean viabilities under 4-hydroxy-tamoxifen and OSU-ERb-12 alone *via* the formula  $\text{Log\_Viability (Bliss)} = \text{Log\_Viability(4-hydroxy-tamoxifen)} + \text{Log\_Viability (OSU-ERb-12)}$ . Interaction at each dose was quantified as the ratio of the predicted viability under the Bliss independence model over the estimated viability under the tested 4-hydroxy-tamoxifen + OSU-ERb-12 combination, with ratios  $>1$  indicating synergy.

Statistical analysis was performed using the R statistical software, including the "survival" package. Summary statistics were computed for demographic variables and expression levels (FPKM), and Spearman correlation coefficients were computed for *ESR1* (ER $\alpha$ ) and *ESR2* (ER $\beta$ ) versus other expression levels. Cox regression was used to calculate the association between overall survival and  $\log_2(1 + \text{FPKM})$  for *ESR1* and *ESR2* expression levels.

## RESULTS

### Selection for Drug-Resistant MCF7 and T47D Cell Lines

We cultured the T47D cell line in the presence of DMSO (control), 4-hydroxy-tamoxifen, fulvestrant, or the CDK4/6i abemaciclib and MCF7 with abemaciclib, at gradually increasing concentrations to select for acquired resistance. With extended exposure of about 8 months, both the cell lines demonstrated decreased sensitivity to the drugs compared with the corresponding parental controls (**Supplemental Figure 1**). As shown in **Supplemental Figure 1**, the resistant cells maintained in drugs containing media and, after several passages over 8 months, demonstrated about 15–110-fold

higher IC<sub>50</sub> values compared with the corresponding control (DMSO) cells. However, in some cases (MCF7-TamR and T47D-TamR) even at high concentrations of the drugs, we did not observe a loss of viability and, therefore, we could not calculate an IC<sub>50</sub> value. Three resistant lines T47D-TamR, T47D-FasR, and, T47D-abemaciclibR cells were maintained in culture with the corresponding drugs at 0.5  $\mu\text{mol/l}$ , and MCF7-abemaciclibR was maintained in abemaciclib at 0.2  $\mu\text{mol/l}$ . Chemical structures of the drugs/inhibitors used in this study are provided in **Supplemental Figure 2**. Lack of activation of the ERE-luciferase reporter vector by overexpressed ER $\alpha$  and ER $\beta$  proteins in 293T cells treated with the inactive chemical analog of OSU-ERb-12 and MCSR-18-006, is shown in **Supplemental Figure 3**. The lack of binding affinity of MCSR-18-006 for ER $\alpha$  and ER $\beta$  proteins as measured by radiolabeled estradiol competition binding assays is shown in **Supplemental Figure 4**.

### *ESR2* and *ESR1* Genes and Their Protein Products Are Differentially Expressed in Various Breast Cancer Cell Lines, and ER $\beta$ Agonists Significantly Enhance ER $\beta$ -Driven ERE-Luciferase Promoter Activity

We assessed the basal expression levels of *ESR2* and *ESR1* in three ER $\alpha$ + breast cancer cell lines (MCF7, T47D, and ZR-75-1) and the derivative endocrine-resistant and CDK4/6i-resistant lines (of MCF7 and T47D) and compared them with those of immortalized mammary epithelial cells (MCF10A) (**Figure 1**) using primers that selectively amplified only the full-length, canonical *ESR2* transcript or that amplified all known splice variants of *ESR2* (**Supplemental Figure 5A**), as well as primers that specifically amplify full-length *ESR1*. The p-values and 95% confidence interval (CI) of corresponding expression data are shown in **Supplemental Table 1**. qRT-PCR data demonstrated a comparable expression of full-length *ESR2* in MCF7 and MCF10A lines (**Figure 1A**, **Supplemental Table 1**). While MCF7-FasR and MCF7-CDK6-O/E cells displayed no significant increase in full-length *ESR2* expression relative to the control MCF10A cells, MCF7-TamR and MCF7-CDK4/6iR cells showed 3.6-fold ( $p = 0.0035$ ) and 6-fold ( $p = 0.0001$ ) higher expression levels, respectively (**Figure 1A** and **Supplemental Table 1**). On the other hand, T47D exhibited a 4.8-fold ( $p = 0.0265$ ) higher expression of *ESR2* compared to MCF10A cells. A significantly higher expression of full-length *ESR2* in T47D-TamR (5.1-fold,  $p = 0.0009$ ) and T47D-CDK4/6iR (5.1-fold,  $p = 0.0075$ ) compared to MCF10A was noted (**Figure 1A** and **Supplemental Table 1**). ZR-75-1 cells displayed the highest level of full-length *ESR2* RNA expression ( $\sim 19$ -fold higher than MCF10A;  $p < 0.01$ ) (**Figure 1A** and **Supplemental Table 1**). Both the TNBC lines had a significantly higher expression of full-length *ESR2* compared with MCF10A (MDA-MB-231: 4.4-fold,  $p < 0.05$ ; MDA-MB-468: 5.2-fold,  $p < 0.01$ ), and these levels were comparable to those in the ER $\alpha$ + MCF7 and T47D breast cancer cell lines.

When we measured expression levels using primers that amplified all the splice isoforms of *ESR2*, the expression levels were significantly higher than MCF10A in most of the cells tested

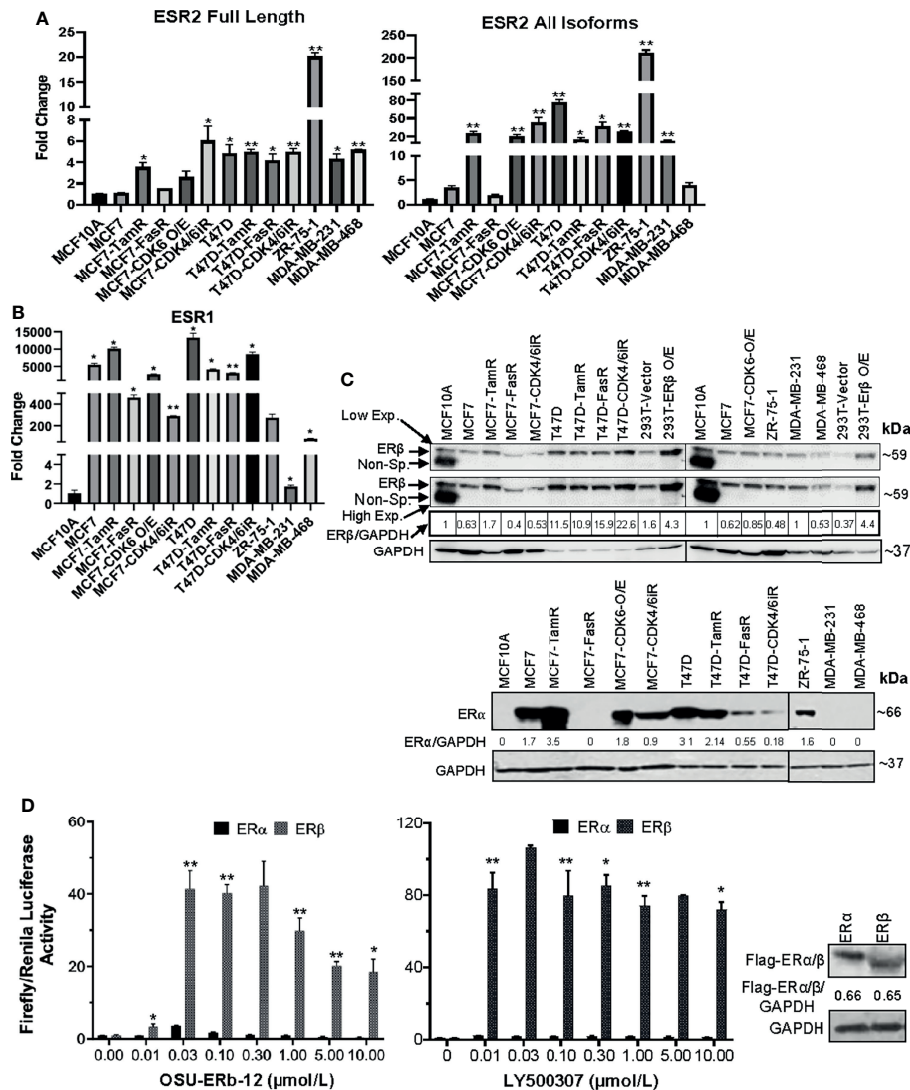


**FIGURE 1 | (A–C)** *ESR1* and *ESR2* genes are differentially expressed in ER $\alpha$ + parental, respective endocrine-resistant, and triple-negative breast cancer cell lines. **(A, B)** Expression of *ESR1* and *ESR2* in immortalized mammary MCF10A, transformed ER $\alpha$ + MCF7 and T47D, endocrine-resistant MCF7-TamR, MCF7-FasR, T47D-TamR, and T47D-FasR, CDK6 overexpressing MCF7 (MCF7-CDK6 O/E), CDK4/6 inhibitor-resistant MCF7 (MCF7-CDK4/6iR) and T47D (T47D-CDK4/6iR), ZR-75-1, and triple-negative breast cancer (TNBC; MDA-MB231, MDA-MB-468, Hs578T) cell lines. Total RNA was isolated from the established cell lines using TRIzol. The expression of each gene was assessed by quantitative RT-PCR (qRT-PCR) performed with the DNase-treated RNA samples using gene-specific primers spanning exon–exon junctions that include large introns in the corresponding genomic sequence to avoid genomic DNA amplification. Gene expression was calculated by the  $\Delta\Delta$ Ct method using GAPDH as an internal control. The expression of each gene is shown as the fold change relative to MCF10A. All reactions were done in triplicate, and the experiment was repeated twice. Data were plotted as mean  $\pm$  SD. **(A)** *ESR2* genes; full length (left) and all isoforms (right). **(B)** *ESR1*. **(C)** Whole-cell lysates were extracted, and immunoblot analyses were performed for ER $\beta$  and GAPDH (loading control) (upper panel), and ER $\alpha$  and GAPDH (lower panel). The intensity of the protein bands was quantified using Image Studio (LiCor) software. Numbers under the lanes of each cell line represent normalized values of the corresponding protein band (ER $\beta$  or ER $\alpha$ ). The normalized band intensity of MCF10A was considered as 1. Immunoblot analyses were repeated twice with corresponding biological replicates. Reproducible results were obtained in each independent experiment. GAPDH, glyceraldehyde-3-phosphate dehydrogenase. For ER $\beta$  (upper panel), two different exposures were provided; low exp.= low exposure; high exp.= higher exposure of the blot. **(D)** ERE-luciferase-driven promoter activity upon treatment with selective ER $\beta$  agonists is significantly higher in ectopically expressing cells with ER $\beta$  compared to that of ER $\alpha$ . HEK293T cells were transfected with c-Flag pcDNA3 (vector control), c-Flag ER $\alpha$  or c-Flag ER $\beta$  in combination with ERE-Luciferase (reporter) and TK-Renilla (pRLTK; internal control) plasmids (as described in *Materials and Methods*). Forty-eight hours after treatment of the cells with ER $\beta$ -specific agonists Renilla and Firefly, luciferase activities were measured using the dual-luciferase reporter assay system. Firefly luciferase was normalized to Renilla Luciferase. Treatment with: OSU-ERb-12 (0–10  $\mu$ mol/l) (left) and LY500307 (0–10  $\mu$ mol/l) (middle). Each assay was performed in triplicate with three experimental replicates (mean  $\pm$  SD, \* $p$  < 0.05, \*\* $p$  < 0.01). The right panel shows equal expressions of ER $\alpha$  and ER $\beta$  as determined by Western blot analysis using the anti-flag antibody. Intensity of Flag-ER $\alpha$ /ER $\beta$  was normalized to GAPDH. The numbers under the immunoblot protein band represent normalized values of the corresponding protein band intensity.

except MCF7, MCF7-FasR, and the TNBC line MDA-MB-468 (**Figure 1A** and **Supplemental Table 1**). About 5,000 ( $p < 0.05$ ) and 12,000-fold ( $p < 0.05$ ) increased *ESR1* expression was noted in MCF7 and T47D cells, respectively, compared to MCF10A (**Figure 1B** and **Supplemental Table 1**).

To check the specificity of the primers to amplify the correct PCR products, we performed agarose gel electrophoresis with the samples of qRT-PCR. Our data showed a single band (**Supplemental Figure 5B**) with correct PCR products that were confirmed by sequencing.

Next, we performed Western blot analyses to evaluate the expression of full-length ER $\beta$  and ER $\alpha$  proteins with the cell lysates (**Figure 1C**). We tested antibodies raised against ER $\beta$  from several different sources including Developmental Studies Hybridoma Bank (CWK-F12), Invitrogen (PPZ0506), and Sigma (clone 68-4). Of these tested antibodies while CWK-F12 and PPZ0506 were specific but only sensitive to the overexpressed (positive control) ER $\beta$  protein, the antibody from Sigma was specific as well as sensitive to ER $\beta$  protein expressed at endogenous levels. As shown in **Figure 1C** (upper panel), all the parental and resistant ER $\alpha$ + cell lines, TNBC lines, and immortalized mammary epithelial cells expressed full-length ER $\beta$ . As expected, our data demonstrated that all the ER $\alpha$ + parental cell lines but none of the TNBC cell lines expressed ER $\alpha$  protein. MCF7-TamR cells expressed more ER $\alpha$  protein than the parental MCF7 cells while MCF7-FasR had no detectable ER $\alpha$  expression. Similarly, T47D-FasR and T47D-CDK4/6iR cells had a lower expression of ER $\alpha$  than the parental T47D cells.

In summary, full-length ER $\beta$  mRNA and protein is expressed in ER $\alpha$ + breast cancer cell lines at levels that are comparable to expression levels in TNBC cell lines, and its expression is preserved in all the resistant derivative cell lines.

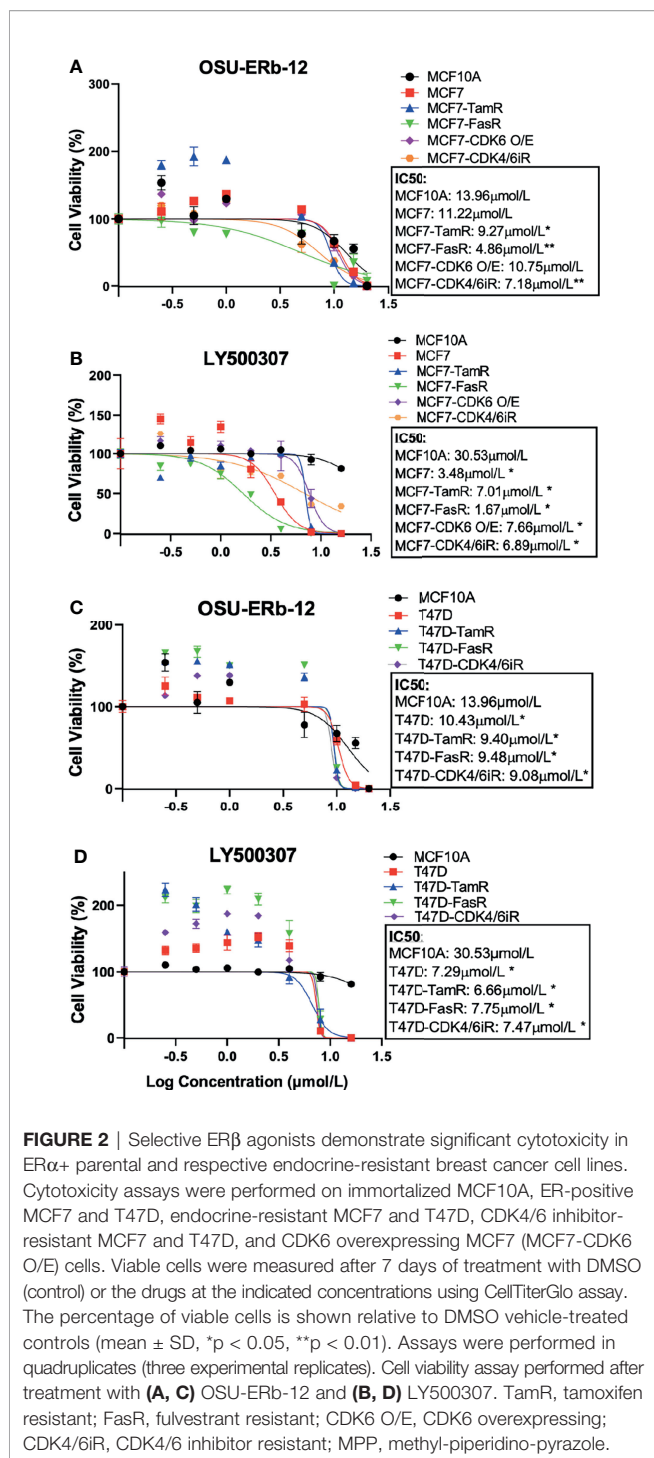
To determine the specificity of ER $\beta$  agonists, we treated HEK293T cells with OSU-ERb-12 or LY500307 (known selective ER $\beta$  agonist) at increasing concentrations following co-transfection with plasmid 3XERE TATA luc, pRLTK, FLAG-ER $\alpha$ , or FLAG-ER $\beta$  (please see *Materials and Methods* for details) and measured luciferase reporter activity (**Figure 1D**). The expression of FLAG-ER $\alpha$  and FLAG-ER $\beta$  proteins was similar as measured by immunoblot for FLAG performed on lysates from the vehicle-treated 293T cells transfected with the corresponding expression plasmids (**Figure 1D**, right panel). Comparison of the induction of luciferase activity demonstrated that ER $\alpha$  exhibited full activity in the presence of 30 nmol/l OSU-ERb-12 and 10 nmol/l LY500307 treatment. Our data showed that luciferase activation by OSU-ERb-12 was significantly increased in the ER $\beta$ -expressing cells as compared to those that expressed ER $\alpha$ . For example, at 30 nmol/l of OSU-ERb-12 there was a ~4-fold ( $p < 0.05$ ) and ~40-fold ( $p < 0.05$ ) increase in luciferase activity in ER $\alpha$  and ER $\beta$  transfected cells, respectively, compared to their corresponding vehicle-treated cells (**Figure 1D**, left panel). There was 10-fold ( $p = 0.0059$ ) higher ERE-LUC activity in ER $\beta$ -overexpressing cells compared to that of ER $\alpha$  by OSU-ERb-12 at 30 nmol/l (**Supplemental Table 2**). Similarly, for LY500307 at 10 nmol/l there was 2.1-fold (maximum induction;  $p < 0.05$ ) activation by ER $\alpha$  and 84-fold

( $p < 0.05$ ) activation by ER $\beta$  compared to the corresponding vehicle-treated samples (**Figure 1D** central panel, **Supplemental Table 2**). At this concentration of LY500307, ER $\beta$  demonstrated 40-fold higher activity ( $p = 0.0038$ ) compared to ER $\alpha$ .

## ER $\beta$ Agonists Are Cytotoxic to ER $\alpha$ + Breast Cancer Cell Lines and They Synergize With ER $\alpha$ + Antagonists

Next, we assessed the viability of parental, endocrine-resistant, CDK4/6i-R MCF7 and T47D, and MCF7-CDK6 O/E cell lines following treatment with ER $\beta$  agonists OSU-ERb-12 and LY500307 (**Figure 2** and **Supplemental Table 3**). We assessed cell viability after 7 days of initial drug exposure using CellTiter-Glo Luminescent Cell Viability Assay. This duration is consistent with that used for toxicity assays with other endocrine agents such as fulvestrant (20, 21). We compared the viability of the drug-treated transformed cell lines to that of MCF10A cells. The IC<sub>50</sub> values for T47D cells (OSU-ERb-12: 10.43  $\mu$ mol/l—**Figure 2C**; LY500307: 7.29  $\mu$ mol/l—**Figure 2D**), tamoxifen- and fulvestrant-resistant MCF7 cells, tamoxifen- and fulvestrant-resistant T47D cells, CDK6-overexpressing MCF7 cells, abemaciclib-resistant MCF7 cells, and abemaciclib-resistant T47D cells were significantly lower than that of MCF10A cells (OSU-ERb-12: 13.96  $\mu$ mol/l; LY500307: 30.53  $\mu$ mol/l; **Figure 2** and **Supplemental Table 3**). Compared to the parental MCF7 cell line, all the resistant lines except MCF7-CDK6 O/E had significantly lower IC<sub>50</sub> values for OSU-ERb-12 (**Figure 2A**). Similarly, all three resistant T47D lines displayed significantly higher sensitivity toward OSU-ERb-12 compared to their parental counterpart (**Figure 2C** and **Supplemental Table 3**).

Despite a high degree of selectivity, we saw some activation of ER $\alpha$  by both ER $\beta$  agonists in our reporter assay (**Figure 1D**). We also observed an increase in viability of ER $\alpha$ + breast cancer cell lines when exposed to low concentrations of both ER $\beta$  agonists. We hypothesized that combining ER $\beta$  agonists with an ER $\alpha$  antagonist would increase their activity and eliminate their stimulatory effects at low concentrations. We tested several ER $\alpha$  antagonists, namely, 4-hydroxy-tamoxifen (selective estrogen receptor modulator), fulvestrant, elacestrant (both selective estrogen receptor degraders/SERDs), and MPP (selective ER $\alpha$  antagonist), at concentrations that fully block ER $\alpha$ , in combination with OSU-ERb-12. As shown in **Figures 3A, B**, in T47D cells, all these ER $\alpha$  antagonists caused a significant reduction in the IC<sub>50</sub> of OSU-ERb-12 and eliminated its stimulatory effects at low concentrations. Of the tested drugs, 4-hydroxy-tamoxifen, when used at a concentration of 0.5  $\mu$ mol/l, displayed the highest efficacy leading to the reduction of IC<sub>50</sub> for OSU-ERb-12 to 1  $\mu$ mol/l from 14.10  $\mu$ mol/l (**Figure 3A** and **Supplemental Table 4**). We further analyzed the validity of the combination treatment of OSU-ERb-12 and 4-hydroxy-tamoxifen using the Bliss independence model (please see *Materials and Methods* for details). Our data demonstrated a significant dose-response with synergy (**Figure 3C** and **Supplemental Table 4**). There was evidence of synergy (the ratio being 1 or above) at all doses for the combination of OSU-ERb-12+Tam. There was no evidence of antagonism at any dose.



We next determined whether OSU-ERb-12 effects are specifically mediated by the ER $\beta$  receptor by comparing the OSU-ERb-12-induced decreases in cell viability to that of an inactive chemical analog MCSR-18-006 that differs at two atoms from OSU-ERb-12 (Supplemental Figure 2). As shown in Figure 3D, in T47D cells, OSU-ERb-12 demonstrated an IC<sub>50</sub> value of 10.41  $\mu$ mol/l that was 3.24-fold lower than for MCSR-18-006 ( $p$  < 0.01). However, in the presence of 4-hydroxy-

tamoxifen (0.5  $\mu$ mol/l) the IC<sub>50</sub> of OSU-ERb-12 was 1.02  $\mu$ mol/l, which was 38.5-fold lower than that of MCSR-18-006 combined with 4-hydroxy-tamoxifen (Figure 3D, right figure; Supplemental Tables 5, 6).

We then tested the viability of both MCF7 and T47D cell lines upon treatment with three other less selective ER $\beta$  agonists, namely, DPN (diarylpropionitrile) (15), AC186 (22), and WAY200070 (23). Our data demonstrated that none of these ER $\beta$  agonists (Supplemental Figure 6) exerted any significant cytotoxic effect on any of the ER $\alpha$ + cell lines.

## Selective ER $\beta$ Agonists Exert Anti-Proliferative and Proapoptotic Effects on ER $\alpha$ + Breast Cancer Cell Lines and Results in Increased Expression of FOXO 1/3 Proteins in ER $\alpha$ + Breast Cancer Cell Lines

Since both the ER $\beta$  agonists reduced the viability of ER $\alpha$ + cell lines, we further examined the mechanism of reduced viability. Both OSU-ERb-12 and LY500307 reduced cell proliferation, induced S phase arrest, and increased apoptosis of MCF7 and T47D cells (Figure 4).

Cell proliferation was reduced by OSU-ERb-12 (10  $\mu$ mol/l) and LY500307 (3  $\mu$ mol/l) in MCF7 cells by 19% ( $p$  = 0.016) and 27% ( $p$  = 0.0028), respectively (Figure 4A and Supplemental Figure 7, Supplemental Table 7). Similarly, in T47D cells OSU-ERb-12 (10  $\mu$ mol/l) and LY500307 (7  $\mu$ mol/l) reduced proliferation by 31% ( $p$  = 0.0074) and 15% ( $p$  = 0.015), respectively (Figure 4A and Supplemental Figure 7, Supplemental Table 7). However, the observation that the ER $\beta$  agonists either significantly increased or did not decrease proliferation at the lower concentration (0.5  $\mu$ mol/l) in both the cell lines explains the increased cell viability observed at lower doses in earlier experiments (Figure 2).

Cell-cycle analysis demonstrated that OSU-ERb-12 treatment (0.5  $\mu$ mol/l) reduced the G<sub>0</sub>/G<sub>1</sub> phase (8.7% decrease  $p$  = 0.02) and increased the S-phase fraction (6.4% increase,  $p$  = 0.0347) of MCF7 as well as in T47D cells (G<sub>0</sub>/G<sub>1</sub>: 6.6% decrease,  $p$  = 0.0036; S-phase: 5.2% increase,  $p$  = 0.0015) (Figure 4B; Supplemental Figure 8; Supplemental Table 8). Similarly, LY500307 at 0.5  $\mu$ mol/l caused a significant reduction in the G<sub>0</sub>/G<sub>1</sub> phase (13% decrease,  $p$  = 0.019) and an increase in the S-phase (7.1% increase,  $p$  = 0.049) of MCF7 as well as T47D cells (G<sub>0</sub>/G<sub>1</sub>: 7.7% decrease,  $p$  = 0.0018; S-phase: 6.2% increase,  $p$  = 0.0004) (Figure 4B; Supplemental Figure 8; Supplemental Table 8). However, at a higher dose (around IC<sub>50</sub>) OSU-ERb-12 demonstrated no significant decrease in the G<sub>0</sub>/G<sub>1</sub> phase nor arrest at the S-phase in both the cell lines—an observation that needs further explanation. Nevertheless, in T47D cells, LY500307 at higher doses (7  $\mu$ mol/l) exhibited a dramatic decrease (34%,  $p$  = 0.0079) in the G<sub>0</sub>/G<sub>1</sub> phase, an increase in apoptotic cells at SubG<sub>0</sub> (5.6%,  $p$  = 0.0068), and an arrest at S (12.8% increase,  $p$  = 0.006) and G<sub>2</sub>/M (7.6% increase,  $p$  = 0.0135) phases. Altogether, these data suggest that treatment with ER $\beta$  agonists causes cell cycle arrest in S and/or G<sub>2</sub>/M phases.

We observed a significant increase in apoptosis of LY500307-treated (7  $\mu$ mol/l) MCF-7 cells (7.7% apoptotic cells,  $p$  = 0.01) compared to the vehicle-treated control (4.2% apoptotic cells).



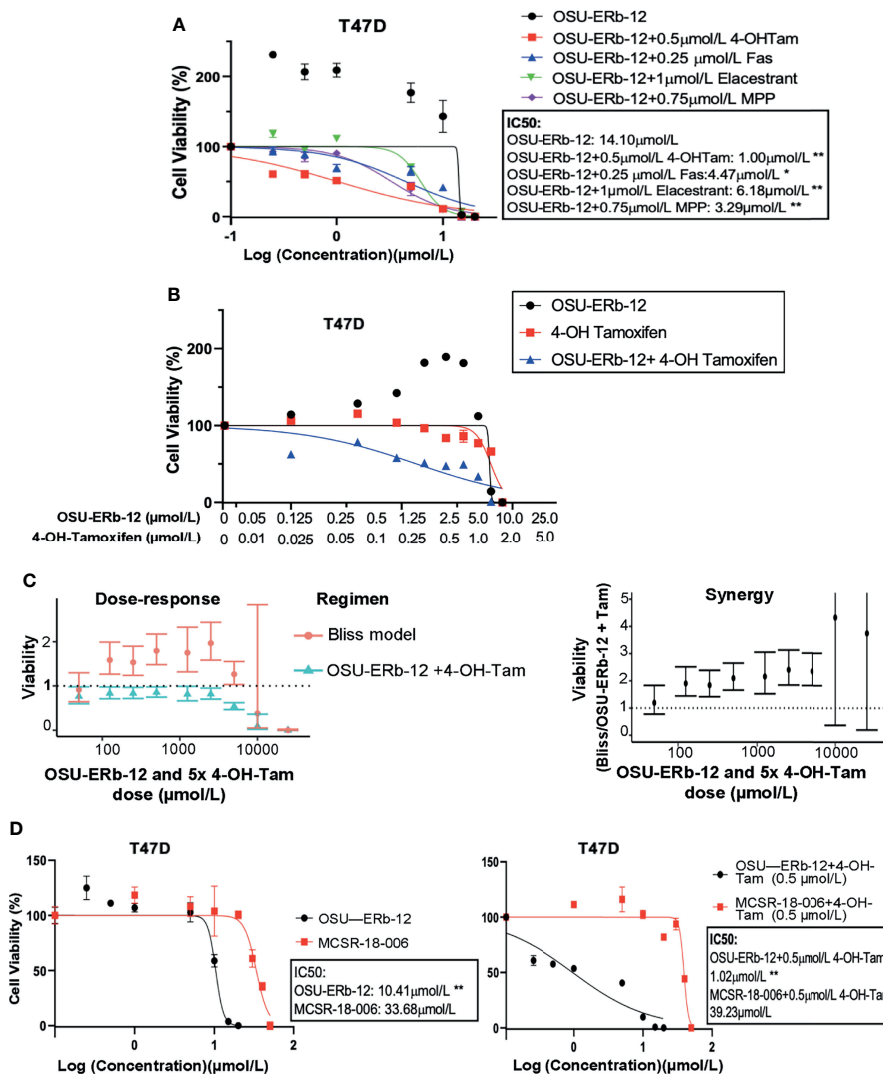


**FIGURE 3 | (A–C)** Combination treatments with selective ER $\beta$  agonists and ER $\alpha$  antagonists demonstrate significant cytotoxicity with reduction in the IC<sub>50</sub> of ER $\alpha$ + breast cancer cell lines. **(A)** T47D treated with OSU-ERb-12 alone and combination with 4-hydroxy tamoxifen, fulvestrant, elacestrant, or MPP or **(B)** OSU-ERb-12 alone, 4-hydroxy tamoxifen alone, and OSU-ERb-12 in combination with 4-hydroxy tamoxifen. **(C)** Linear mixed models were fit for viability versus regimen for each dose, with random effects accounting for within-batch correlation. Bliss independence model predictions are products of fitted values for 4-hydroxy tamoxifen and OSU-ERb-12. Error bars are 95% confidence intervals. **(Left)** The ratio of predicted viabilities (Bliss independence/combination 4-hydroxy tamoxifen + OSU-ERb-12) quantifies interaction, with ratios >1 indicating synergy. Error bars are 95% confidence intervals **(right)**. **(D)** T47D treated with OSU-ERb-12 or MCSR-18-006 (left), and combination of OSU-ERb-12/MCSR-18-006 with 4-hydroxy tamoxifen (right). Viable cells were measured after 7 days of treatment with DMSO (control) or the drugs at the indicated concentrations using CellTiterGlo assay. The percentage of viable cells is shown relative to DMSO vehicle-treated controls (mean  $\pm$  SD, \* $p$  < 0.05, \*\* $p$  < 0.01). Assays were performed in quadruplicates (three experimental replicates).

We did not observe a statistically significant increase in apoptosis of MCF7 cells treated with OSU-ERb-12. We noticed a significant increase in apoptosis of T47D cells treated with 10  $\mu$ mol/l OSU-ERb-12 (13%,  $p$  = 0.03), 0.5  $\mu$ mol/l LY500307 (10.1%,  $p$  = 0.003), and 7  $\mu$ mol/L LY500307 (11.1%,  $p$  = 0.0005) apoptotic cells, respectively as compared to the vehicle-treated control (3.2%) (**Figure 4C**; **Supplemental Figure 9**; **Supplemental Table 9**).

Next, we tested the efficacy of OSU-ERb-12 and LY500307 in reducing colony formation of MCF7 and T47D cells. Colony-

forming ability was significantly reduced upon treatment with both the agonists (**Figure 5A** and **Supplemental Table 10**). In comparison with vehicle-treated cells, OSU-ERb-12 suppressed colony formation of MCF7 cells by 14% ( $p$  = 0.05) and 44% ( $p$  = 0.002) and LY500307 by 79% ( $p$  = 0.003) and 100% ( $p$  = 0.0007) at 3 and 5  $\mu$ mol/l, respectively. Similarly, the reduction in colony formation in T47D with OSU-ERb-12 was 64.5% (5  $\mu$ mol/l;  $p$  = 0.011). With LY500307, colony formation was reduced by 19.9% (3  $\mu$ mol/l;  $p$  = 0.015) and 95% (5  $\mu$ mol/l;  $p$  = 0.005). However, there was no significant reduction of colony formation in T47D

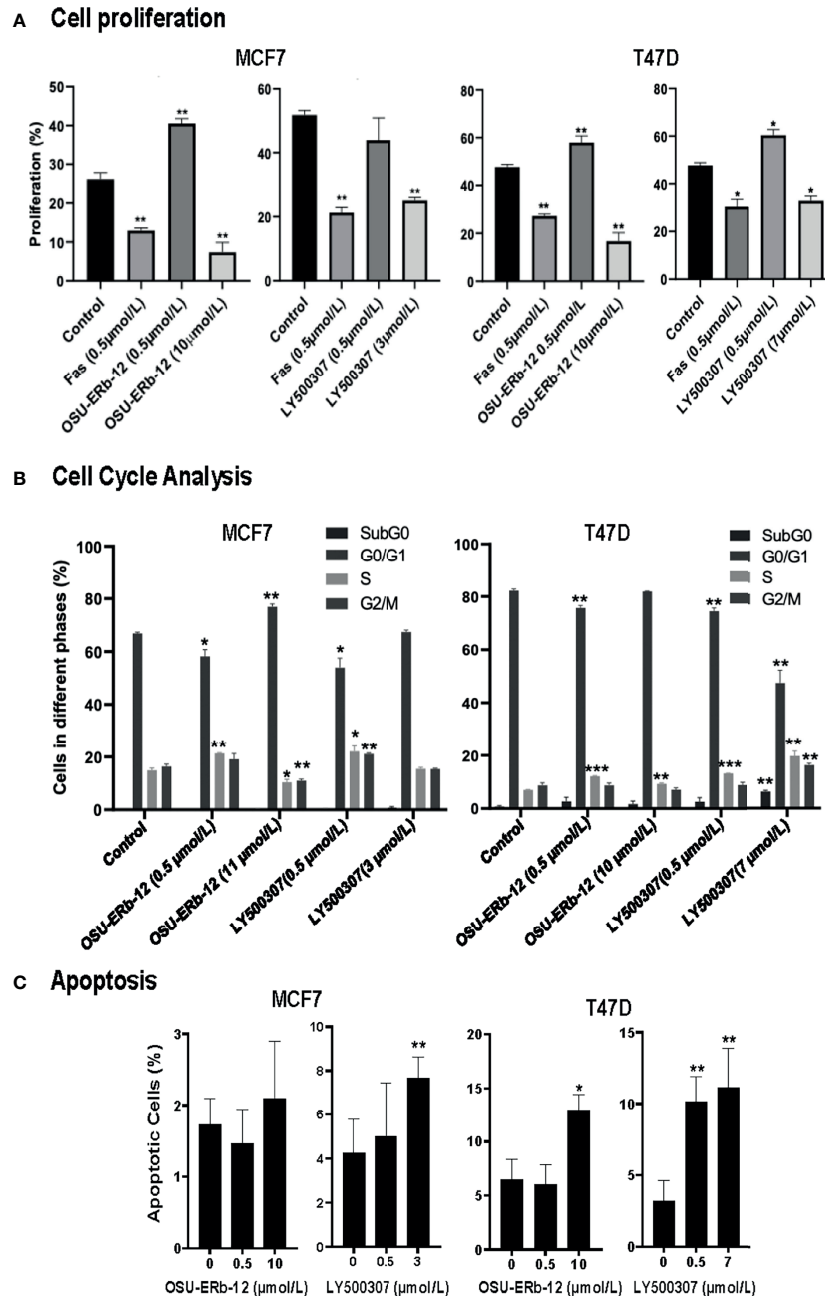


**FIGURE 4** | Cell proliferation, cell cycle, and apoptosis are affected upon treatment of ER $\alpha$ + breast cancer cells with ER $\beta$ -specific agonists, OSU-ERb-12, and LY500307. MCF7 and T47D cells ( $0.5 \times 10^6$ ) were seeded on 100-mm dishes in phenol red free DMEM containing charcoal-stripped FBS and treated with the drugs as indicated. **(A)** A representative diagram of the cell proliferation profile in drug-treated cells. Cells were treated with DMSO (control), FAS (fulvestrant; negative control), OSU-ERb-12, or LY500307 for 72 h, harvested, and stained following protocol for the Click-IT EdU Alexa Fluor 647 Kit (Invitrogen C10424). Cell proliferation was analyzed *via* flow cytometry on a BD FACSCalibur Flow Cytometer. Each assay was performed in triplicate and repeated twice. Data were plotted as mean  $\pm$  SD (\* $p < 0.05$ , \*\* $p < 0.01$ ). **(B)** A representative diagram depicting the cell-cycle profile in drug-treated cells. Cells treated with DMSO (control), OSU-ERb-12, or LY500307 for 72 h at the indicated concentrations were harvested on ice, fixed, washed, and incubated with propidium iodide and RNase A followed by cell-cycle analysis on a flow cytometer. Each assay was performed in triplicate and repeated twice. Data were plotted as mean  $\pm$  SD (\* $p < 0.05$ , \*\* $p < 0.01$ , \*\*\* $p < 0.001$ ). **(C)** A representative diagram depicting the apoptosis profile in drug-treated cells. Cells treated with DMSO (control), OSU-ERb-12, or LY500307 for 48 h at the indicated concentrations were harvested on ice, washed, and processed according to the manufacturer's protocol (TUNEL Assay Kit-BrdU-Red; Abcam) followed by analysis on a BD FACSCalibur Flow Cytometer. Each experiment was repeated twice. Data presented are mean  $\pm$  SD (\* $p < 0.05$ , \*\* $p < 0.01$ ). In all assays, results shown are pooled averages across biological repeats.

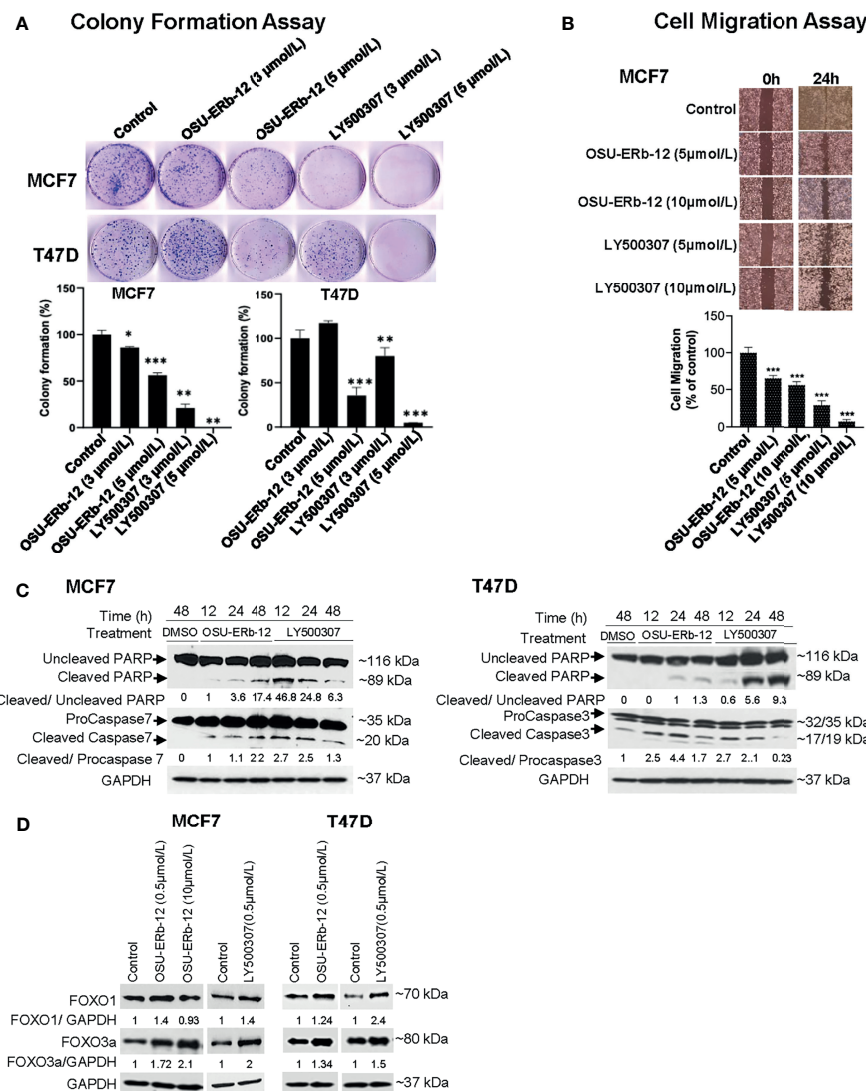


**FIGURE 5** | Treatment with ER $\beta$ -specific agonists OSU-ERb-129 and LY500307 promotes anticancer effects in ER $\alpha$ + breast cancer lines *in vitro*. **(A)** Colony formation. Colonies were stained with crystal violet and counted. The percentage of colonies present in each treatment is shown relative to DMSO vehicle-treated controls. Data are from three independent experiments and presented as mean  $\pm$  SD; \* $p$  < 0.05, \*\* $p$  < 0.01, \*\*\* $p$  < 0.001;  $n$  = 3. **(B)** Cell migration. Cell migration was determined using the wound-healing assay. The percentage of the filled area is calculated, normalized to DMSO-treated control, and presented as mean  $\pm$  SD from three independent experiments; mean  $\pm$  SD; \* $p$  < 0.05, \*\* $p$  < 0.01, \*\*\* $p$  < 0.001;  $n$  = 3. **(C)** Enhanced cleavage of PARP-1, and activation of caspases 3 and 7 in ER $\alpha$ + breast cancer cells upon treatment with ER $\beta$  agonists. Western blot analyses were performed using specific antibodies in whole-cell lysates prepared from OSU-ERb-12- and LY500307-treated cells as indicated. Similar results were obtained in different batches of cells treated with OSU-ERb-12 and LY500307. Numbers under the lanes are the quantitative representation of the intensity of the normalized bands. The signal in each band was quantified using Image Studio (LiCor) software. **(D)** Enhanced expression of FOXO1 and FOXO3a proteins in ER $\alpha$ + breast cancer cells upon treatment with ER $\beta$  agonists. Western blot analyses were performed using specific antibodies in whole cell lysates prepared from cells treated for 7 days with OSU-ERb-12 or LY500307. Similar results were obtained with different batches of cells treated with OSU-ERb-12 or LY500307. Numbers under the lanes represent corresponding normalized band intensity of the respective proteins. Image Studio (LiCor) software was used to quantify the intensity of the protein bands.

treated with 3  $\mu$ mol/l OSU-ERb-12 (**Figure 5A** and **Supplemental Table 10**).

We then performed wound healing assays to investigate whether OSU-ERb-12 and LY500307 treatments could lead to the reduction of migratory properties of breast cancer cells. As shown in **Figure 5B**, there was a significant decrease in the cell motility in the MCF7 cell line in the presence of both the

agonists. Treatment with OSU-ERb-12 inhibited MCF7 cell migration by 34.7% (5  $\mu$ mol/l;  $p$  = 0.0004) and 42.9% (10  $\mu$ mol/l;  $p$  = 0.0026) and LY500307 by 70.2% (5  $\mu$ mol/l;  $p$  < 0.0001) and 91.9% (10  $\mu$ mol/l;  $p$  < 0.0001) (**Figure 5B** and **Supplemental Table 11**).

To elucidate the underlying mechanism of ER $\beta$  agonist-mediated cell death, we measured the levels of activated

executioner caspases by Western blot analysis. As MCF7 cells do not express caspase 3 (24), we measured caspase 7 levels in this cell line. Robust activation of the effector caspases 7 (MCF7) or 3 (T47D) resulted within 12 h of treatment of cells with both the agonists. The effect persisted at least up to 48 h (Figure 5C). In contrast, in vehicle-treated cells increased caspase cleavage was not detected. A similar increase in the proteolysis of their substrate PARP-1 was noted in ER $\beta$  agonist-treated cells (Figure 5C).

It has been demonstrated that ER $\beta$  suppresses tumor growth and induces apoptosis by augmenting the transcription of the tumor-suppressor genes *FOXO1* and *FOXO3* in prostate cancer (25). Therefore, we determined their expression levels in ER $\beta$  agonist-treated breast cancer cells. As shown in Figure 5D, both *FOXO1* and *FOXO3a* protein levels were increased in OSU-ERb-12- and LY500307-treated MCF7 and T47D cell lines.

## ER $\beta$ Expression in Human Breast Cancer Samples

Previous studies suggested that, distinct from ER $\alpha$ , ER $\beta$  inhibits transcription from promoters that incorporate estrogen response-tetradecanoyl phorbol ester (ERE-AP1) composite response elements (13). We hypothesized that the ER $\beta$ /*ESR2* mRNA expression levels in ER $\alpha$ + human breast cancer samples would negatively correlate with those of genes with promoters that contain ERE-AP1 response elements and that there would be a positive association between *ESR2* mRNA expression levels and overall survival.

Thirty-seven patients with metastatic ER $\alpha$ +/*HER2*- breast cancer were included in this study. Demographic and clinical characteristics are displayed in Supplemental Table 12. All the patients in this cohort were female with a median age of 56 years (range 27–78). The patients were predominantly Caucasian (35, 95%), and most women were postmenopausal (23, 66%).

The objective was to determine the mRNA expression levels of the genes which are targets of ER-AP1-mediated transcription and AP1-independent ER mediated transcription including *CCND1*, *MYC*, *IGF-1*, *Bcl-2*, *MMP-1*, *FN1*, *IGFBP-4*, *E2F4*, *CXCL12*, *PGR*, (ERE-AP1 dependent) *EBAG9*, and *TRIM25* (canonical palindromic ERE dependent) and to correlate these with *ESR1* and *ESR2*. We found by RNA-seq analysis that the expression of the cyclin D1 gene, the classic target of estrogen-stimulated transcription through an AP1 response element, negatively correlated with that of ER $\beta$ /*ESR2* as measured using the Spearman correlation coefficient ( $\rho = -0.45$ ,  $p = 0.005$ ) (Figure 6A and Supplemental Table 13). ER $\beta$ /*ESR2* expression was also negatively correlated with that of ER $\alpha$ /*ESR1* ( $\rho = -0.35$ ,  $p = 0.033$ ). However, ER $\beta$ /*ESR2* mRNA expression positively correlated with that of *IGFBP4* ( $\rho = 0.58$ ,  $p < 0.001$ ) and *CXCL12* ( $\rho = 0.54$ ,  $p < 0.001$ ) (Figure 6B and Supplemental Table 13). The univariate Cox proportional hazard estimate for overall survival by *ESR2* expression was 0.54 (95% CI 0.06, 5.22), suggesting a positive trend that did not reach statistical significance in this numerically limited cohort (Figure 6C). The RNA-seq data reported in this paper are available at the Gene Expression Omnibus database (accession

no. GSE198545) at: [https://urldefense.com/v3/\\_\\_https://www.ncbi.nlm.nih.gov/geo/query/acc.cgi?acc=GSE198545\\_\\_;!!KGKeukY!kY3\\_5pg7Oz9dTPBWxvXq1t1PTXXZY07hndoLq0XVgXcesakiudG7GxZuDQamvwLNorY\\$](https://urldefense.com/v3/__https://www.ncbi.nlm.nih.gov/geo/query/acc.cgi?acc=GSE198545__;!!KGKeukY!kY3_5pg7Oz9dTPBWxvXq1t1PTXXZY07hndoLq0XVgXcesakiudG7GxZuDQamvwLNorY$).

## DISCUSSION

The ER $\alpha$  subtype constitutes 70% of all breast cancers. Annually about 600,000 breast cancer-related death occurs worldwide (1). Although metastatic ER $\alpha$ + breast cancer is initially treated with estrogen deprivation or ER $\alpha$  blockade, endocrine resistance eventually entails a change of therapy. The advent of CDK4/6 inhibitors such as palbociclib (26, 27), ribociclib (28), and abemaciclib (29, 30) has doubled progression-free survival when used in combination with endocrine agents. However, resistance to CDK4/6 inhibitors is an increasing clinical challenge (31). Also, the duration of response to second-line endocrine therapies is generally short. After the exhaustion of endocrine treatment, chemotherapy remains the only treatment option. Therefore, there is an urgent need for tolerable therapies to prolong overall survival with better quality of life for advanced ER $\alpha$ + breast cancer patients.

Accumulating evidence suggests that while ER $\alpha$  is prooncogenic in the mammary gland, ER $\beta$  plays a tumor-suppressor role in different cancers including breast cancer (32, 33). The efficacy of selective ER $\beta$  agonists such as LY500307 has been previously described in preclinical models of TNBC (34), melanoma (34), glioblastoma multiforme (35), and prostate cancer (36). However, there has been limited study of the role of ER $\beta$  in estrogen receptor  $\alpha$ -positive breast cancer. One reason is that for this particular indication a high degree of selectivity for ER $\beta$  over ER $\alpha$  would be required. Our institution recently developed a highly selective ER $\beta$  agonist: OSU-ERb-12 (16). We confirmed the selectivity of this compound using ERE-luciferase promoter assays showing 10-fold higher induction upon treatment of ER $\beta$ -overexpressing cells.

Although previous preclinical studies have mostly focused on TNBC, we observed that ER $\beta$  was expressed (both RNA and protein level) in ER $\alpha$ + breast cancer cell lines at levels that were not significantly different from those in TNBC cell lines (Figures 1A–C). Endocrine and CDK4/6 resistant derivatives of these ER $\alpha$ + cell lines had comparable or higher expression compared to the parental cell lines. These observations, therefore, are in line with the potential for efficacy in ER $\alpha$ + breast cancer.

We showed that OSU-ERb-12, like the control compound LY500307, exerted significant cytotoxicity toward MCF7 and T47D ER $\alpha$ + breast cancer cell lines with IC50 values that were lower compared to immortal mammary epithelial cells (MCF10A). Furthermore, OSU-ERb-12 exhibited cytotoxicity toward the corresponding endocrine- and CDK4/6 inhibitor-resistant derivative lines of MCF7 and T47D with either similar or even significantly lower IC50 values, demonstrating its therapeutic efficacy toward both treatment-naïve and -resistant ER $\alpha$ + breast cancer cells. Furthermore, we demonstrated that these effects are ER $\beta$  specific using a close structural analog that

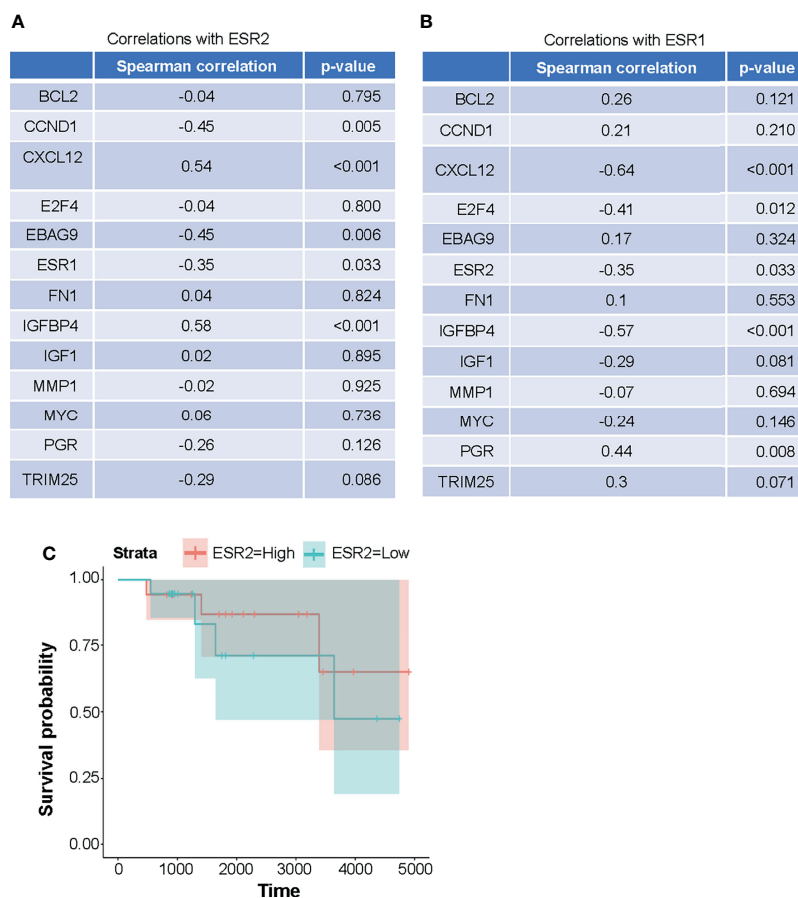


**FIGURE 6 | (A, B)** Expression of the genes that are targets of ER-AP1-mediated transcription and AP1-independent ERE-mediated transcription in metastatic HER2-negative ER+ breast cancer patients is positively correlated with *ESR2*. **(A)** expression of *ESR2* is positively correlated with *CXCL12* and *IGFBP4* expressions and negatively correlated with *CCND1*, *EBAG9*, and *ESR1* expressions. **(B)** *ESR1* expressions is positively correlated with *PGR* expressions and negatively correlated with *CXCL12*, *E2F4*, *IGFBP4*, and *ESR2* expressions. Expression levels (FPKM) and Spearman correlation coefficients were computed for *ESR1* and *ESR2* expressions versus other gene expression levels. **(C)** Overall survival was not significantly correlated with the expression of *ESR2* in the HER2-negative ER $\alpha$ + metastatic breast cancer patient cohort, although there was a trend toward a positive correlation. *ESR2* was dichotomized relative to the median expression level and tested via the log-rank test ( $p = 0.6$ ). Cox proportional hazards regression on the continuous expression levels yielded similar results (HR 0.6,  $p = 0.7$ ).

lacks ER $\beta$  agonist activity and was many-fold less cytotoxic than the active compound. Also, we showed that less specific ER $\beta$  agonists have much lower potency for inhibiting ER $\alpha$ + cell lines. The reason for this is unclear but could be due to off-target activation of ER $\alpha$ .

At lower concentrations of OSU-ERb-12 and LY500307, there was an increase in cell viability. We hypothesized that this may be due to ER $\alpha$  activation, given the large molar excess of ER $\alpha$  receptors over ER $\beta$  receptors in ER $\alpha$ + breast cancer cell lines. This prompted us to investigate the cytotoxic efficacy of OSU-ERb-12 in combination with clinically available potent ER $\alpha$  antagonists. In the combination studies, tamoxifen showed maximum inhibitory effect with a 14-fold reduction of IC50 value compared with OSU-ERb-12 alone. Using the Bliss Independence model, we found a synergistic interaction between tamoxifen and OSU-ERb-12 at all the doses used in the study. These data would suggest that if clinically used, OSU-

ERb-12 should be administered in combination with tamoxifen or other selective estrogen receptor modulators. The strategy of using an endocrine agent, such as tamoxifen, with a sensitizing targeted agent in the endocrine-resistant setting has been used successfully in clinical trials (37).

Of note, the cellular 50% inhibitory concentrations were many-fold higher than the cellular 50% effective concentration for activation of a canonical palindromic ERE response element. There are many potential explanations for this. Firstly, inhibition of viability may only be achieved when the majority of available receptors are activated by the ligand, for example possibly at the EC90–100 concentration range. Secondly, the EC50 concentration represents transcriptional activation at a palindromic estrogen response element with optimal configuration and spacing of the half binding sites. Depending on the configuration of the EREs in promoters, EC50 may be higher. Of note, ligand-ER-DNA interactions, including the stoichiometry and affinity of the

ligand for the ligand-binding domain, are dependent on the spacing and orientation of ERE-binding sites as well as flanking sequences (38–40). Thirdly, cytotoxicity may be independent of transcription but rather may rely on ligand-induced protein–protein interactions that may also modulate ligand binding affinity (41).

Our study demonstrated the efficacy of ER $\beta$  agonists in attenuating cell proliferation, cell migration, and colony formation as well as inducing cell-cycle arrest and apoptosis of ER $\alpha$ + breast cancer cell lines. However, differential effects in inducing apoptosis in MCF7 and T47D cells suggest that these two ER $\beta$  agonists OSU-ERb-12 and LY500307 may exert distinct anticancer effects. Ligand-specific effects of ER $\beta$  have been previously described by other groups (42). Also, we showed that ER $\beta$  agonist-treated MCF7 and T47D cells exhibited activation of effector caspases 7/3 and cleavage of PARP as well, which are markers of apoptosis.

FOXO proteins act as tumor suppressors in a variety of cancers including breast cancer (43, 44). Previous studies have shown that ER $\beta$  upregulates the expression of FOXO transcription factors in preclinical models of prostate cancer (25, 45, 46). Our data demonstrated a significantly higher expression of both FOXO1 and FOXO3a proteins in ER $\beta$  agonist-treated cells. Thus, induction of FOXO proteins may be one of the mechanism(s) by which OSU-ER-12 exhibits its tumor-suppressor activity. Further confirmation of the necessity of FOXO transcription factor upregulation for the efficacy of ER $\beta$  agonists will be required.

Given the tumor-suppressor activity of ER $\beta$ , we hypothesized that its expression would be positively associated with the overall survival of metastatic breast cancer patients. In the present study, we showed that in a cohort of 37 metastatic breast cancer patients there was a trend of increased overall survival in *ESR2*-high-expressing patients compared to *ESR2*-low-expressing patients. However, these data are not statistically significant in this small cohort of patients. Further analysis of a larger cohort is warranted. Previous studies had suggested that ER $\beta$  might antagonize the transcriptional upregulation of genes that incorporate composite estrogen-phorbol ester response elements such as *CCND1* (47–49). In our cohort of patients, we found that the expression of *CCND1* mRNA, a typical estrogen-stimulated target gene, is negatively correlated with the expression of *ESR2* mRNA.

In conclusion, we have provided sufficient evidence that OSU-ERb-12 could be a potential candidate compound for its inhibitory activity toward ER $\alpha$ + breast cancer. These interesting results warrant further work, especially in regard to the mechanism of tumor suppression by ER $\beta$  and confirmation of its efficacy as a therapeutic strategy using *in vivo* preclinical models.

## REFERENCES

- Sung H, Ferlay J, Siegel RL, Laversanne M, Soerjomataram I, Jemal A, et al. Global Cancer Statistics 2020: GLOBOCAN Estimates of Incidence and Mortality Worldwide for 36 Cancers in 185 Countries. *CA Cancer J Clin* (2021) 71(3):209–49. doi: 10.3322/caac.21660
- Gong Y, Liu YR, Ji P, Hu X, Shao ZM. Impact of Molecular Subtypes on Metastatic Breast Cancer Patients: A SEER Population-Based Study. *Sci Rep* (2017) 7:45411. doi: 10.1038/srep45411

## DATA AVAILABILITY STATEMENT

The raw data supporting the conclusions of this article will be made available by the authors, without undue reservation.

## AUTHOR CONTRIBUTIONS

MAC and JD conceived the project. JD, CCC, BR, and MAC designed the experiments. BR, ML, DGS, SDS, and MAC helped recruit the patients to the protocol under which the patient data were collected. JD, NW, JMM, PS, MS, JJD, DGS, and MK performed the experiments and analyzed the data. JD and MAC wrote the manuscript. All authors contributed to the article and approved the submitted version.

## FUNDING

This publication [or project] was supported, in part, by the National Center for Advancing Translational Sciences of the National Institutes of Health under Grant Number KL2TR002734. OSU-ERb-12 and MCSR-18-006 were synthesized by the Medicinal Chemistry Shared Resource, and the corresponding mass spectral data were obtained by the Proteomics Shared Resource, both of which are part of The Ohio State University Comprehensive Cancer Center and supported by NCI/NIH Grant P30CA016058. This work was also supported by the Drug Development Institute within The Ohio State University Comprehensive Cancer Center and Pelotonia. Additionally, this work was supported by a grant from the National Comprehensive Cancer Network. The content is solely the responsibility of the authors and does not necessarily represent the official views of the National Institutes of Health.

## ACKNOWLEDGMENTS

We would like to thank the Comprehensive Cancer Center, Arthur G. James Cancer Hospital, and Richard Solove Research Institute at the Ohio State University Wexner Medical Center for supporting the study. We also would like to acknowledge Jackie Sharpnack for administrative support. This manuscript is available for preprint: doi: <https://doi.org/10.1101/2022.01.14.476328>

## SUPPLEMENTARY MATERIAL

The Supplementary Material for this article can be found online at: <https://www.frontiersin.org/articles/10.3389/fonc.2022.857590/full#supplementary-material>

- Li Z, Razavi P, Li Q, Toy W, Liu B, Ping C, et al. Loss of the FAT1 Tumor Suppressor Promotes Resistance to CDK4/6 Inhibitors *via* the Hippo Pathway. *Cancer Cell* (2018) 34(6):893–905. doi: 10.1016/j.ccell.2018.11.006
- Cornell L, Wander SA, Visal T, Wagle N, Shapiro GI. MicroRNA-Mediated Suppression of the TGF-Beta Pathway Confers Transmissible and Reversible CDK4/6 Inhibitor Resistance. *Cell Rep* (2019) 26(10):2667–80. doi: 10.1016/j.celrep.2019.02.023
- Pandey K, Park N, Park KS, Hur J, Cho YB, Kang M, et al. Combined CDK2 and CDK4/6 Inhibition Overcomes Palbociclib Resistance in Breast Cancer by

- Enhancing Senescence. *Cancers (Basel)* (2020) 12(12):3566. doi: 10.3390/cancers12123566
6. Russo J, Russo IH. The Role of Estrogen in the Initiation of Breast Cancer. *J Steroid Biochem Mol Biol* (2006) 102(1-5):89–96. doi: 10.1016/j.jsbmb.2006.09.004
  7. Mal R, Magner A, David J, Datta J, Vallabhaneni M, Kassem M, et al. Estrogen Receptor Beta (ERbeta): A Ligand Activated Tumor Suppressor. *Front Oncol* (2020) 10:587386. doi: 10.3389/fonc.2020.587386
  8. Pinton G, Thomas W, Bellini P, Manente AG, Favoni RE, Harvey BJ, et al. Estrogen Receptor Beta Exerts Tumor Repressive Functions in Human Malignant Pleural Mesothelioma via EGFR Inactivation and Affects Response to Gefitinib. *PLoS One* (2010) 5(11):e14110. doi: 10.1371/journal.pone.0014110
  9. Ma L, Liu Y, Geng C, Qi X, Jiang J. Estrogen Receptor Beta Inhibits Estradiol-Induced Proliferation and Migration of MCF-7 Cells Through Regulation of Mitofusin 2. *Int J Oncol* (2013) 42(6):1993–2000. doi: 10.3892/ijo.2013.1903
  10. Pinton G, Zonca S, Manente AG, Cavaletto M, Borroni E, Daga A, et al. SIRT1 at the Crossroads of AKT1 and ERbeta in Malignant Pleural Mesothelioma Cells. *Oncotarget* (2016) 7(12):14366–79. doi: 10.18632/oncotarget.7321
  11. Deroo BJ, Buensuceso AV. Minireview: Estrogen Receptor-Beta: Mechanistic Insights From Recent Studies. *Mol Endocrinol* (2010) 24(9):1703–14. doi: 10.1210/me.2009-0288
  12. Huang J, Li X, Maguire CA, Hilf R, Bambara RA, Muyan M. Binding of Estrogen Receptor Beta to Estrogen Response Element *in Situ* is Independent of Estradiol and Impaired by its Amino Terminus. *Mol Endocrinol* (2005) 19(11):2696–712. doi: 10.1210/me.2005-0120
  13. Chang EC, Charn TH, Park SH, Helfferich WG, Komm B, Katzenellenbogen JA, et al. Estrogen Receptors Alpha and Beta as Determinants of Gene Expression: Influence of Ligand, Dose, and Chromatin Binding. *Mol Endocrinol* (2008) 22(5):1032–43. doi: 10.1210/me.2007-0356
  14. Kuiper GGJM, Enmark E, Peltö-Huikko M, Nilsson S, Gustafsson JA. Cloning of a Novel Estrogen Receptor Expressed in Rat Prostate and Ovary. *Proc Natl Acad Sci USA* (1996) 93:5925–30. doi: 10.1073/pnas.93.12.5925
  15. Harrington WR, Sheng S, Barnett DH, Petz LN, Katzenellenbogen JA, Katzenellenbogen BS. Activities of Estrogen Receptor Alpha- and Beta-Selective Ligands at Diverse Estrogen Receptor Gene Sites Mediating Transactivation or Transrepression. *Mol Cell Endocrinol* (2003) 206(1-2):13–22. doi: 10.1016/s0303-7207(03)00255-7
  16. Sedlak D, Wilson TA, Tjarks W, Radomska HS, Wang H, Kolla JN, et al. Structure-Activity Relationship of Para-Carborane Selective Estrogen Receptor Beta Agonists. *J Med Chem* (2021) 64(13):9330–53. doi: 10.1021/acs.jmedchem.1c00555
  17. Beretta GL, Corno C, Zaffaroni N, Perego P. Role of FoxO Proteins in Cellular Response to Antitumor Agents. *Cancers (Basel)* (2019) 11(1):90–115. doi: 10.3390/cancers11010090
  18. Fan M, Yan PS, Hartman-Frey C, Chen L, Paik H, Oyer SL, et al. Diverse Gene Expression and DNA Methylation Profiles Correlate With Differential Adaptation of Breast Cancer Cells to the Antiestrogens Tamoxifen and Fulvestrant. *Cancer Res* (2006) 66(24):11954–66. doi: 10.1158/0008-5472.CAN-06-1666
  19. Yang C, Li Z, Bhatt T, Dickler M, Giri D, Scaltriti M, et al. Acquired CDK6 Amplification Promotes Breast Cancer Resistance to CDK4/6 Inhibitors and Loss of ER Signaling and Dependence. *Oncogene* (2017) 36(16):2255–64. doi: 10.1038/onc.2016.379
  20. Hoffmann J, Bohlmann R, Heinrich N, Hofmeister H, Kroll J, Kunzer H, et al. Characterization of New Estrogen Receptor Destabilizing Compounds: Effects on Estrogen-Sensitive and Tamoxifen-Resistant Breast Cancer. *J Natl Cancer Inst* (2004) 96(3):210–8. doi: 10.1093/jnci/djh022
  21. Mishra AK, Abrahamsson A, Dabrosin C. Fulvestrant Inhibits Growth of Triple Negative Breast Cancer and Synergizes With Tamoxifen in ERalpha Positive Breast Cancer by Up-Regulation of ERbeta. *Oncotarget* (2016) 7(35):56876–88. doi: 10.18632/oncotarget.10871
  22. George S, Petit GH, Gouras GK, Brundin P, Olsson R. Nonsteroidal Selective Androgen Receptor Modulators and Selective Estrogen Receptor Beta Agonists Moderate Cognitive Deficits and Amyloid-Beta Levels in a Mouse Model of Alzheimer's Disease. *ACS Chem Neurosci* (2013) 4(12):1537–48. doi: 10.1021/cn400133s
  23. Hughes ZA, Liu F, Platt BJ, Dwyer JM, Pulicicchio CM, Zhang G, et al. WAY-200070, a Selective Agonist of Estrogen Receptor Beta as a Potential Novel Anxiolytic/Antidepressant Agent. *Neuropharmacology* (2008) 54(7):1136–42. doi: 10.1016/j.neuropharm.2008.03.004
  24. Janicke RU. MCF-7 Breast Carcinoma Cells do Not Express Caspase-3. *Breast Cancer Res Treat* (2009) 117(1):219–21. doi: 10.1007/s10549-008-0217-9
  25. Nakajima Y, Akaogi K, Suzuki T, Osakabe A, Yamaguchi C, Sunahara N, et al. Estrogen Regulates Tumor Growth Through a Nonclassical Pathway That Includes the Transcription Factors ERbeta and KLF5. *Sci Signal* (2011) 4(168):ra22. doi: 10.1126/scisignal.2001551
  26. Finn RS, Crown JP, Lang I, Boer K, Bondarenko IM, Kulyk SO, et al. The Cyclin-Dependent Kinase 4/6 Inhibitor Palbociclib in Combination With Letrozole Versus Letrozole Alone as First-Line Treatment of Oestrogen Receptor-Positive, HER2-Negative, Advanced Breast Cancer (PALOMA-1/TRIO-18): A Randomised Phase 2 Study. *Lancet Oncol* (2015) 16(1):25–35. doi: 10.1016/S1470-2045(14)71159-3
  27. Montagna E, Colleoni M. Hormonal Treatment Combined With Targeted Therapies in Endocrine-Responsive and HER2-Positive Metastatic Breast Cancer. *Ther Adv Med Oncol* (2019) 11:1758835919894105. doi: 10.1177/1758835919894105
  28. Hortobagyi GN, Stemmer SM, Burris HA, Yap YS, Sonke GS, Paluch-Shimon S, et al. Ribociclib as First-Line Therapy for HR-Positive, Advanced Breast Cancer. *N Engl J Med* (2016) 375(18):1738–48. doi: 10.1056/NEJMoa1609709
  29. Goetz MP, Toi M, Campone M, Sohn J, Paluch-Shimon S, Huober J, et al. MONARCH 3: Abemaciclib As Initial Therapy for Advanced Breast Cancer. *J Clin Oncol* (2017) 35(32):3638–46. doi: 10.1200/JCO.2017.75.6155
  30. Xu XQ, Pan XH, Wang TT, Wang J, Yang B, He QJ, et al. Intrinsic and Acquired Resistance to CDK4/6 Inhibitors and Potential Overcoming Strategies. *Acta Pharmacol Sin* (2021) 42(2):171–8. doi: 10.1038/s41401-020-0416-4
  31. Osborne CK, Schiff R. Mechanisms of Endocrine Resistance in Breast Cancer. *Annu Rev Med* (2011) 62:233–47. doi: 10.1146/annurev-med-070909-182917
  32. Murphy LC, Leygue E. The Role of Estrogen Receptor-Beta in Breast Cancer. *Semin Reprod Med* (2012) 30(1):5–13. doi: 10.1055/s-0031-1299592
  33. Dey P, Barros RP, Warner M, Strom A, Gustafsson JA. Insight Into the Mechanisms of Action of Estrogen Receptor Beta in the Breast, Prostate, Colon, and CNS. *J Mol Endocrinol* (2013) 51(3):T61–74. doi: 10.1038/onc.2013.384
  34. Zhao L, Huang S, Mei S, Yang Z, Xu L, Zhou N, et al. Pharmacological Activation of Estrogen Receptor Beta Augments Innate Immunity to Suppress Cancer Metastasis. *Proc Natl Acad Sci USA* (2018) 115(16):E3673–E81. doi: 10.1073/pnas.1803291115
  35. Sareddy GR, Li X, Liu J, Viswanadhapalli S, Garcia L, Gruslova A, et al. Selective Estrogen Receptor Beta Agonist LY500307 as a Novel Therapeutic Agent for Glioblastoma. *Sci Rep* (2016) 6:24185. doi: 10.1038/srep24185
  36. Roehrborn CG, Spann ME, Myers SL, Serviss CR, Hu L, Jin Y. Estrogen Receptor Beta Agonist LY500307 Fails to Improve Symptoms in Men With Enlarged Prostate Secondary to Benign Prostatic Hypertrophy. *Prostate Cancer Prostatic Dis* (2015) 18(1):43–8. doi: 10.1038/pcan.2014.43
  37. Bachelot T, Bourcier C, Cropet C, Ray-Coquard I, Ferrero JM, Freyer G, et al. Randomized Phase II Trial of Everolimus in Combination With Tamoxifen in Patients With Hormone Receptor-Positive, Human Epidermal Growth Factor Receptor 2-Negative Metastatic Breast Cancer With Prior Exposure to Aromatase Inhibitors: A GINECO Study. *J Clin Oncol* (2012) 30(22):2718–24. doi: 10.1200/JCO.2011.39.0708
  38. Anolik JH, Klinge CM, Bambara RA, Hilf R. Differential Impact of Flanking Sequences on Estradiol- vs 4-Hydroxytamoxifen-Liganded Estrogen Receptor Binding to Estrogen Responsive Element DNA. *J Steroid Biochem Mol Biol* (1993) 46(6):713–30. doi: 10.1016/0960-0760(93)90312-k
  39. Anolik JH, Klinge CM, Hilf R, Bambara RA. Cooperative Binding of Estrogen Receptor to DNA Depends on Spacing of Binding Sites, Flanking Sequence, and Ligand. *Biochemistry* (1995) 34(8):2511–20. doi: 10.1021/bi00008a015
  40. Klinge CM, Studinski-Jones AL, Kulakosky PC, Bambara RA, Hilf R. Comparison of Tamoxifen Ligands on Estrogen Receptor Interaction With Estrogen Response Elements. *Mol Cell Endocrinol* (1998) 143(1-2):79–90. doi: 10.1016/s0303-7207(98)00130-0
  41. Anolik JH, Klinge CM, Brolly CL, Bambara RA, Hilf R. Stability of the Ligand-Estrogen Receptor Interaction Depends on Estrogen Response Element Flanking Sequences and Cellular Factors. *J Steroid Biochem Mol Biol* (1996) 59(5-6):413–29. doi: 10.1016/s0960-0760(96)00129-x
  42. Paech K, Webb P, Kuiper GG, Nilsson S, Gustafsson J, Kushner PJ, et al. Differential Ligand Activation of Estrogen Receptors ERalpha and ERbeta at

- AP1 Sites. *Science* (1997) 277(5331):1508–10. doi: 10.1126/science.277.5331.1508
43. Yang JY, Zong CS, Xia W, Yamaguchi H, Ding Q, Xie X, et al. ERK Promotes Tumorigenesis by Inhibiting FOXO3a via MDM2-Mediated Degradation. *Nat Cell Biol* (2008) 10(2):138–48. doi: 10.1038/ncb1676
44. Zou Y, Tsai WB, Cheng CJ, Hsu C, Chung YM, Li PC, et al. Forkhead Box Transcription Factor FOXO3a Suppresses Estrogen-Dependent Breast Cancer Cell Proliferation and Tumorigenesis. *Breast Cancer Res* (2008) 10(1):R21. doi: 10.1186/bcr1872
45. Dey P, Strom A, Gustafsson JA. Estrogen Receptor Beta Upregulates FOXO3a and Causes Induction of Apoptosis Through PUMA in Prostate Cancer. *Oncogene* (2014) 33(33):4213–25. doi: 10.1186/bcr1872
46. Nakajima Y, Osakabe A, Waku T, Suzuki T, Akaogi K, Fujimura T, et al. Estrogen Exhibits a Biphasic Effect on Prostate Tumor Growth Through the Estrogen Receptor Beta-KLF5 Pathway. *Mol Cell Biol* (2016) 36(1):144–56. doi: 10.1128/MCB.00625-15
47. Maruyama S, Fujimoto N, Asano K, Ito A. Suppression by Estrogen Receptor Beta of AP-1 Mediated Transactivation Through Estrogen Receptor Alpha. *J Steroid Biochem Mol Biol* (2001) 78(2):177–84. doi: 10.1016/s0960-0760(01)00083-8
48. Liu MM, Albanese C, Anderson CM, Hilty K, Webb P, Uht RM, et al. Opposing Action of Estrogen Receptors Alpha and Beta on Cyclin D1 Gene Expression. *J Biol Chem* (2002) 277(27):24353–60. doi: 10.1074/jbc.M201829200
49. Chewchuk S, Guo B, Parissenti AM. Alterations in Estrogen Signalling Pathways Upon Acquisition of Anthracycline Resistance in Breast Tumor Cells. *PLoS One* (2017) 12(2):e0172244. doi: 10.1371/journal.pone.0172244

**Conflict of Interest:** The authors declare that the research was conducted in the absence of any commercial or financial relationships that could be construed as a potential conflict of interest.

**Publisher's Note:** All claims expressed in this article are solely those of the authors and do not necessarily represent those of their affiliated organizations, or those of the publisher, the editors and the reviewers. Any product that may be evaluated in this article, or claim that may be made by its manufacturer, is not guaranteed or endorsed by the publisher.

Copyright © 2022 Datta, Willingham, Manouchehri, Schnell, Sheth, David, Kassem, Wilson, Radomska, Coss, Bennett, Ganju, Sardesai, Lustberg, Ramaswamy, Stover and Cherian. This is an open-access article distributed under the terms of the Creative Commons Attribution License (CC BY). The use, distribution or reproduction in other forums is permitted, provided the original author(s) and the copyright owner(s) are credited and that the original publication in this journal is cited, in accordance with accepted academic practice. No use, distribution or reproduction is permitted which does not comply with these terms.